universe

MDPI

Article

Explaining the Muon $g-2$ Anomaly in Deflected AMSB for NMSSM

Lijun Jia, Zhuang Li and Fei Wang *

School of Physics, Zhengzhou University, Zhengzhou 450001, China; 202012132012247@gs.zzu.edu.cn (L.J.J.); lizhuang@gs.zzu.edu.cn (Z.L.)

* Correspondence: feiwang@zzu.edu.cn

Abstract: We propose to embed the General NMSSM (Next-to-Minimal Supersymmetric Standard Model) into the deflected AMSB (Anomaly Mediated Supersymmetry Breaking) mechanism with Yukawa/gauge deflection contributions. After the integration of the heavy messenger fields, the analytical expressions of the relevant soft SUSY breaking spectrum for General NMSSM at the messenger scale can be calculated. We find that successful EWSB (Electroweak Symmetry Breaking) and realistic low energy NMSSM spectrum can be obtained in some parameter regions. In addition, we find that the muon $g-2$ anomaly and electron $g-2$ anomaly (for positive central value electron $g-2$ experimental data) can be jointly explained to 1σ and 2σ range, respectively. The Z_3 invariant NMSSM, which corresponds to $\xi_F = 0$ in our case, can also jointly explain the muon and electron anomaly to 1σ and 2σ range, respectively.

Keywords: deflected AMSB; general NMSSM; muon $g-2$ anomaly

check for updates

Citation: Jia, L.; Li, Z.; Wang, F. Explaining the Muon $g-2$ Anomaly in Deflected AMSB for NMSSM. *Universe* **2023**, *9*, 214. https://doi.org/10.3390/universe9050214

Academic Editor: Maxim Y. Khlopov

Received: 1 April 2023
Revised: 19 April 2023
Accepted: 28 April 2023
Published: 29 April 2023

1. Introduction

The Standard Model (SM) of particle physics is very successful in explaining the vast experimental measurements up to the electroweak (EW) scale, including the discovery of Higgs boson by the Large Hadron Collider (LHC) [1,2]. However, it still has many theoretical and aesthetic problems, for example, the quadratic divergence of the fundamental Higgs scalar mass, the dark matter (DM) puzzle, and the origin of baryon asymmetry in the universe. In addition, it has been known for a long time that the theoretical prediction of the muon anomalous magnetic moment $a_\mu \equiv (g-2)_\mu/2$ for SM has subtle deviations from the experimental values. In fact, combining the recent reported E989 muon $g-2$ measurement with the previous BNL result [3,4], the updated world average experimental value of a_μ is given by [5]

$$a_\mu^{\mathrm{FNAL+BNL}} = (11,659,206.2 \pm 4.1) \times 10^{-10}\,, \tag{1}$$

which has a 4.2σ deviation from the SM prediction [6]

$$\Delta a_\mu^{\mathrm{FNAL+BNL}} = (25.1 \pm 5.9) \times 10^{-10}\,. \tag{2}$$

In addition to the reported muon $g-2$ anomaly, the experimental data on electron $g-2$ also reported some deviations from the SM predictions. From the measurement of the fine structure constant $\alpha_{\mathrm{em}}(Cs)$ by the Berkeley experiment using ^{133}Cs atoms [7], the experimental value on electron $g-2$ by [8] has a 2.4σ deviation from the SM prediction [9]

$$\Delta a_e^{\mathrm{Exp-SM}} = a_e^{\mathrm{Exp}} - a_e^{\mathrm{SM}}(^{133}Cs) = (-8.8 \pm 3.6) \times 10^{-13}\,, \tag{3}$$

with the center value taking the negative sign. Such a result is not consistent with the most accurate 2020 measurement using ^{87}Rb atoms [10], which reported a 1.6σ deviation from SM prediction

$$\Delta a_e^{\mathrm{Exp-SM}} = a_e^{\mathrm{Exp}} - a_e^{\mathrm{SM}}(^{87}Rb) = (4.8 \pm 3.0) \times 10^{-13}\,, \tag{4}$$

with the center value taking the positive sign. Although the deviation of electron $g-2$ is still controversial, its possible theoretical implications should not be overlooked. The previous problems and anomalies strongly indicate that SM should not be the whole story and it only acts as the low energy effective theory of some new physics beyond the SM.

Various new physics models had been proposed to deal with the problems that bother the SM. Among them, low-energy supersymmetry (SUSY) is the most attractive one, which can accommodate almost all the solutions of such problems together in a single framework. In particular, the discovered 125 GeV Higgs scalar lies miraculously in the small '$115-135$' GeV window predicted by the low energy SUSY, which is a strong hint of weak scale SUSY. So, if low energy SUSY is indeed the new physics beyond the SM, it should account for the new muon $g-2$ anomaly. SUSY explanations of the muon $g-2$ anomaly can be seen in the literatures [11–38]. Furthermore, there have already been several discussions offering combined explanations of the experimental results for electron and muon $g-2$ anomaly in the SUSY framework [39–47]. On the other hand, it is rather non-trivial for the low-energy SUSY breaking spectrum to be consistent with recent experimental bounds, for example, the LHC exclusion bounds and DM null search results. As the low-energy soft SUSY breaking parameters are fully determined by the predictive SUSY breaking mechanism, their intricate structures can be a consequence of the mediation mechanism of SUSY breaking in the UV theory, for example, the well-motivated anomaly mediated SUSY breaking (AMSB) [48,49] mechanism.

Minimal AMSB, which is determined solely by the F-term VEV of the compensator superfield F_ϕ (its value is approximately equal to the gravitino mass $m_{3/2}$), is insensitive to its UV theory [50] and predicts a flavor conservation soft SUSY breaking spectrum. Unfortunately, negative slepton squared masses are predicted and the minimal scenario must be extended. Although there are many possible ways to tackle such tachyonic slepton masses problems, the most elegant solution from an aesthetic point of view is the deflected AMSB (dAMSB) [51–55] scenario, which adopts non-trivially an additional messenger sector to deflect the AMSB trajectory and push the negative slepton squared masses to positive values by additional gauge mediation contributions.

Next-to-Minimal Supersymmetric Standard Model (NMSSM) [56,57] can elegantly solve the μ problem that bothers the Minimal Supersymmetric Standard Model (MSSM) with an additional singlet sector. In addition, with additional tree-level contributions or through doublet-singlet mixing, NMSSM can accommodate easily the discovered 125 GeV Higgs boson mass. However, soft SUSY breaking parameters of low-energy NMSSM from a typical SUSY breaking mechanism, such as gauge-mediated SUSY breaking (GMSB) [58,59], are always bothered by the requirement to achieve successful EWSB with suppressed trilinear couplings A_κ, A_λ and m_S^2, rendering the model building non-trivial [60]. Such difficulties always persist in ordinary AMSB-type scenarios. We find that the phenomenologically interesting NMSSM spectrum with successful EWSB can be successfully generated by combining both AMSB and GMSB-type contributions. In addition, the discrepancy between the theoretical predictions for the muon (and electron) anomalous magnetic momentum and the experiments can be explained in such model.

This paper is organized as follows. In Section 2, we propose our model and discuss the general expression for soft SUSY parameters. The soft SUSY parameters for General NMSSM are given in our scenario. The relevant numerical results are studied in Section 3. Section 4 contains our conclusions.

2. Soft SUSY Breaking Parameters of NMSSM from Deflected AMSB

We know that NMSSM is well motivated theoretically to solve the $\mu - B\mu$ problem. By imposing the discrete Z_3 symmetry, a bare μ term is forbidden in the NMSSM. An effective μ_{eff} parameter can be generated by

$$\mu_{eff} \equiv \lambda \langle s \rangle, \tag{5}$$

after the S field acquires the VEV $\langle s \rangle$, which lies of order the electroweak scale and breaks the Z_3 symmetry. The Z_3 invariant superpotential couplings are given by [56,57]

$$W_{Z_3NMSSM} \quad = \quad W_{MSSM}|_{\mu=0} + \lambda S H_u H_d + \frac{\kappa}{3} S^3 \,, \tag{6}$$

with

$$W_{MSSM}|_{\mu=0} = y^u_{ij} Q_{L,i} H_u U^c_{L,j} - y^d_{ij} Q_{L,i} H_d D^c_{L,j} - y^e_{ij} L_{L,i} H_d E^c_{L,j} \,. \tag{7}$$

The soft SUSY breaking parameters are given as

$$\mathcal{L}^{soft}_{Z_3NMSSM} = \mathcal{L}^{soft}_{MSSM}|_{B=0} - \left(A_\lambda \lambda S H_u H_d + A_\kappa \frac{\kappa}{3} S^3 \right) - m_S^2 |S|^2 \,. \tag{8}$$

The breaking of Z_3 discrete symmetry in the scale-invariant NMSSM is bothered with the domain-wall problem, creating unacceptably large anisotropies of the CMB and spoiling successful BBN predictions. In addition, discrete global symmetry cannot be exact at the Planck scale and may be violated by Planck scale suppressed gravitational interactions. Although one can find complicated solutions to such difficulties, it is interesting to go beyond the Z_3 invariant scheme and adopt the general NMSSM (GNMSSM) to evade the previous problems. In fact, effective GNMSSM can also be generated from scale invariant NMSSM if one introduces, in the Jordan frame, a $\chi H_u H_d$ term in the frame function that couples to the curvature.

GNMSSM is the most general single gauge singlet chiral superfield S extension of MSSM, including the most general renormalizable couplings in the superpotential and the corresponding soft SUSY breaking terms in $\mathcal{L}_{soft}$. On the other hand, as noted previously, GNMSSM does not adopt the Z_3 symmetry, which can contain the Z_3 breaking terms [56,57]

$$W_{\not{Z}_3NMSSM} \quad = \xi_F S + \tfrac{1}{2} \mu' S^2 + \hat{\mu} H_u H_d \,. \tag{9}$$

So, the general superpotential of GNMSSM contains

$$W_{GNMSSM} \supseteq W_{Z_3NMSSM} + W_{\not{Z}_3NMSSM} \,, \tag{10}$$

with the corresponding new terms of soft SUSY breaking parameter

$$-\mathcal{L} \supseteq m_3^2 H_u H_d + \frac{1}{2} m_S'^2 S^2 + \xi_S S + h.c. \,. \tag{11}$$

Such low-energy soft SUSY breaking parameters are determined by the corresponding SUSY breaking mechanism in the UV-completion theory [58,61–63]. However, it is rather non-trivial to generate the phenomenological desirable low-energy soft SUSY breaking spectrum from UV theory. In fact, null search results of sparticles with 139 fb^{-1} of data at the (13 TeV) LHC by the ATLAS and CMS collaborations [64] suggest that the low-energy SUSY spectrum should have an intricate pattern. For example, the first two generation squarks need to be heavy to avoid the stringent constraints from LHC. To explain the muon $g-2$ anomaly, light electroweakinoes and sleptons are always preferred. On the other hand, the discovered 125 GeV Higgs boson by both the ATLAS and CMS collaborations of LHC may indicate stop masses of order 5∼10 TeV or TeV scale stops with large trilinear coupling A_t. As light stops can be preferred to keep electroweak naturalness, large trilinear

coupling A_t is, therefore, needed to accommodate the 125 GeV Higgs. We know that minimal GMSB predicts vanishing A_t at the messenger scale and introducing messenger–matter interactions will sometimes be bothered with additional flavor constraints. So, we propose to generate the phenomenological desirable low-energy NMSSM soft spectrum in the predictive AMSB-type framework with additional Yukawa mediation contributions.

As the slepton sector of NMSSM is the same as that of MSSM, the prediction of the NMSSM soft spectrum from AMSB is still bothered with the tachyonic slepton problem. The most elegant solution to such a problem is to add an additional messenger sector, which can deflect the AMSB trajectory properly so that the slepton squared masses can be pushed to positive values. The minimal version of deflected AMSB in NMSSM, which is a straightforward extension of ordinary minimal deflected AMSB for MSSM, adopts no additional interactions other than that between the spurion field and the messengers. However, it is still problematic in realizing successful EWSB and triggering a non-vanishing $\langle s \rangle$, as the necessary condition $A_\kappa^2 \gtrsim 9m_S^2$ [56,57] can not be satisfied easily. In addition, our numerical results indicate that the corresponding SUSY contributions to muon $g-2$ anomaly is very small for the few survived parameter points. So, additional coupling terms in the superpotential involving the singlet S and messengers can be introduced to bring new Yukawa deflection contributions to the soft SUSY breaking spectrum and alter those parameters relevant for EWSB.

To evade unwanted mixing between the singlet chiral field S and the spurion field X, we adopt the following form of superpotential at the messenger scale

$$W \supseteq W_{Z_3NMSSM} + \sum_{i=1}^{2N} \lambda_{X;i} X(\bar{\Psi}_i \Psi_i) + \sum_{j=1}^{N} \lambda_{S;j} S(\bar{\Psi}_j \Psi_{j+1}) + W(X)\,, \tag{12}$$

with the coupling form first proposed in [65] for GMSB embedding of NMSSM.

The soft SUSY breaking parameters in deflected AMSB can be given by mixed anomaly mediation and gauge mediation contributions. When the renormalization group equation (RGE) evolves down below the messenger thresholds, the anomaly mediation contributions will receive threshold corrections after integrating out the messenger fields. The wavefunction renormalization approach [66,67] can also be used in deflected AMSB [68,69] to keep track of supersymmetry-breaking effects with a manifestly supersymmetric formalism and obtain the soft SUSY breaking spectrum. In deflected AMSB, the messenger threshold M_{mess} and the RGE scale μ in the wavefunction superfield and gauge kinetic superfield can be replaced by the following combinations involving the spurious chiral fields X

$$M_{mess} \to \sqrt{\frac{X^\dagger X}{\phi^\dagger \phi}}\,, \quad \mu \to \frac{\mu}{\sqrt{\phi^\dagger \phi}}\,, \tag{13}$$

which, after substituting the F-term VEV of X and ϕ, can obtain the soft SUSY breaking parameters. Below the messenger scale, the messenger superfields will be integrated out and will deflected the trajectory from ordinary AMSB trajectory. The superpotential for pseudo-moduli superfield $W(X)$ can be fairly generic and leads to a deflection parameter of either sign given by

$$d \equiv \frac{F_X}{M F_\phi} - 1. \tag{14}$$

After integrating out the heavy messengers, we can obtain the soft SUSY breaking spectrum at the messenger scale. The soft gaugino masses at the messenger scale can be given by

$$M_i(M_{mess}) \quad = \quad g_i^2 \left(\frac{F_\phi}{2} \frac{\partial}{\partial \ln \mu} - \frac{d F_\phi}{2} \frac{\partial}{\partial \ln |X|} \right) \frac{1}{g_i^2}(\mu, |X|, T)\,, \tag{15}$$

with

$$\frac{\partial}{\partial \ln |X|} g_i(\alpha; |X|) = \frac{\Delta b_i}{16\pi^2} g_i^3 \,, \tag{16}$$

The trilinear soft terms can be determined by the wavefunction renormalization factors

$$\begin{aligned} A_0^{ijk} \equiv \frac{A_{ijk}}{y_{ijk}} &= \sum_i \left(-\frac{F_\phi}{2} \frac{\partial}{\partial \ln \mu} + dF_\phi \frac{\partial}{\partial \ln X} \right) \ln[Z_i(\mu, X, T)] \,, \\ &= \sum_i \left(-\frac{F_\phi}{2} G_i^- + dF_\phi \frac{\Delta G_i}{2} \right) . \end{aligned} \tag{17}$$

In our convention, the anomalous dimension are expressed in the holomorphic basis [70]

$$G^i \equiv \frac{dZ_{ij}}{d \ln \mu} \equiv -\frac{1}{8\pi^2} \left(\frac{1}{2} d^i_{kl} \lambda^*_{ikl} \lambda_{jmn} Z^{-1*}_{km} Z^{-1*}_{ln} - 2c^i_r Z_{ij} g_r^2 \right). \tag{18}$$

and $\Delta G \equiv G^+ - G^-$ the discontinuity of anomalous dimension across the messenger threshold. Here, '$G^+(G^-)$' denote the values of anomalous dimension above (below) the messenger threshold, respectively. The soft scalar masses are given by

$$m^2_{soft} = -\left| -\frac{F_\phi}{2} \frac{\partial}{\partial \ln \mu} + dF_\phi \frac{\partial}{\partial \ln X} \right|^2 \ln[Z_i(\mu, X, T)] \,, \tag{19}$$

$$= -\left(\frac{F_\phi^2}{4} \frac{\partial^2}{\partial (\ln \mu)^2} + \frac{d^2 F_\phi^2}{4} \frac{\partial}{\partial (\ln |X|)^2} - \frac{dF_\phi^2}{2} \frac{\partial^2}{\partial \ln |X| \partial \ln \mu} \right) \ln[Z_i(\mu, X, T)]. \tag{20}$$

From the previous analytic expressions, we can calculate the soft SUSY breaking parameters for MSSM at the messenger scale. The gaugino masses are calculated to be

$$M_i = F_\phi \frac{\alpha_i(\mu)}{4\pi} (b_i - d\Delta b_i) \,, \tag{21}$$

with the corresponding beta function $(b_1\,, b_2\,,\, b_3) = (\frac{33}{5},\, 1, -3)$ [71] and the changes of beta function for the gauge couplings

$$\Delta(b_1\,, b_2\,,\, b_3) = (2N,\, 2N,\, 2N), \tag{22}$$

with N representing the family of messengers in (12).

The trilinear soft terms are calculated to be

$$\begin{aligned} A_t &= \frac{F_\phi}{16\pi^2} \left[\tilde{G}_{y_t} \right] , \\ A_b &= \frac{F_\phi}{16\pi^2} \left[\tilde{G}_{y_b} \right] , \\ A_\tau &= \frac{F_\phi}{16\pi^2} \left[\tilde{G}_{y_\tau} \right] , \\ A_\lambda &= \frac{F_\phi}{16\pi^2} \left[\tilde{G}_\lambda - d\Delta \tilde{G}_\lambda \right] , \\ A_\kappa &= \frac{F_\phi}{16\pi^2} \left[\tilde{G}_\kappa - d\Delta \tilde{G}_\kappa \right] , \\ \frac{\xi_S}{\xi_F} &= \frac{1}{2} \frac{m'^2_S}{\mu'} = \frac{1}{3} A_\kappa \,, \\ \frac{m_3^2}{\hat{\mu}} &= \frac{F_\phi}{16\pi^2} \left[\tilde{G}_{\hat{\mu}} \right] , \end{aligned} \tag{23}$$

with

$$\begin{aligned}
\tilde{G}_\lambda &= 4\lambda^2 + 2\kappa^2 + 3y_t^2 + 3y_b^2 + y_\tau^2 - (3g_2^2 + \frac{3}{5}g_1^2)\,, \\
\tilde{G}_\kappa &= 6\lambda^2 + 6\kappa^2\,, \\
\tilde{G}_{y_t} &= \lambda^2 + 6y_t^2 + y_b^2 - (\frac{16}{3}g_3^2 + 3g_2^2 + \frac{13}{15}g_1^2)\,, \\
\tilde{G}_{y_b} &= \lambda^2 + y_t^2 + 6y_b^2 + y_\tau^2 - (\frac{16}{3}g_3^2 + 3g_2^2 + \frac{7}{15}g_1^2)\,, \\
\tilde{G}_{y_\tau} &= \lambda^2 + 3y_b^2 + 4y_\tau^2 - (3g_2^2 + \frac{9}{5}g_1^2)\,, \\
\tilde{G}_{\hat{\mu}} &= 3y_t^2 + 3y_b^2 + y_\tau^2 - (3g_2^2 + \frac{3}{5}g_1^2)\,,
\end{aligned} \tag{24}$$

and the discontinuity of the Yukawa beta functions across the messenger threshold

$$\begin{aligned}
\Delta\tilde{G}_\lambda &= 5\sum_{j=1}^{N}\lambda_{S;j}^2\,, \\
\Delta\tilde{G}_\kappa &= 15\sum_{j=1}^{N}\lambda_{S;j}^2\,.
\end{aligned} \tag{25}$$

The sfermion masses can be calculated to be

$$\begin{aligned}
m_{H_u}^2 &= \frac{F_\phi^2}{16\pi^2}\left[\frac{3}{2}G_2\alpha_2^2 + \frac{3}{10}G_1\alpha_1^2\right] + \frac{F_\phi^2}{(16\pi^2)^2}\left[\lambda^2\tilde{G}_\lambda + 3y_t^2\tilde{G}_{y_t}\right]\,, \\
m_{H_d}^2 &= \frac{F_\phi^2}{16\pi^2}\left[\frac{3}{2}G_2\alpha_2^2 + \frac{3}{10}G_1\alpha_1^2\right] + \frac{F_\phi^2}{(16\pi^2)^2}\left[\lambda^2\tilde{G}_\lambda + 3y_b^2\tilde{G}_{y_b} + y_\tau^2\tilde{G}_{y_\tau}\right]\,, \\
m_{\tilde{Q}_{L;1,2}}^2 &= \frac{F_\phi^2}{16\pi^2}\left[\frac{8}{3}G_3\alpha_3^2 + \frac{3}{2}G_2\alpha_2^2 + \frac{1}{30}G_1\alpha_1^2\right]\,, \\
m_{\tilde{U}_{L;1,2}^c}^2 &= \frac{F_\phi^2}{16\pi^2}\left[\frac{8}{3}G_3\alpha_3^2 + \frac{8}{15}G_1\alpha_1^2\right]\,, \\
m_{\tilde{D}_{L;1,2}^c}^2 &= \frac{F_\phi^2}{16\pi^2}\left[\frac{8}{3}G_3\alpha_3^2 + \frac{2}{15}G_1\alpha_1^2\right]\,, \\
m_{\tilde{L}_{L;1,2}}^2 &= \frac{F_\phi^2}{16\pi^2}\left[\frac{3}{2}G_2\alpha_2^2 + \frac{3}{10}G_1\alpha_1^2\right]\,, \\
m_{\tilde{E}_{L;1,2}^c}^2 &= \frac{F_\phi^2}{16\pi^2}\frac{6}{5}G_1\alpha_1^2\,,
\end{aligned} \tag{26}$$

with

$$\begin{aligned}
G_i &= 2Nd^2 + 4Nd - b_i\,, \\
(b_1, b_2, b_3) &= (\frac{33}{5}, 1, -3)\,.
\end{aligned} \tag{27}$$

For the third generation, the sfermion masses are given by

$$\begin{aligned}
m^2_{\tilde{Q}_{L,3}} &= m^2_{\tilde{Q}_{L;1,2}} + F^2_\phi \frac{1}{(16\pi^2)^2}\left[y_t^2 \tilde{G}_{y_t} + y_b^2 \tilde{G}_{y_b}\right], \\
m^2_{\tilde{U}^c_{L,3}} &= m^2_{\tilde{U}^c_{L;1,2}} + F^2_\phi \frac{1}{(16\pi^2)^2}\left[2y_t^2 \tilde{G}_{y_t}\right], \\
m^2_{\tilde{D}^c_{L,3}} &= m^2_{\tilde{D}^c_{L;1,2}} + F^2_\phi \frac{1}{(16\pi^2)^2}\left[2y_b^2 \tilde{G}_{y_b}\right], \\
m^2_{\tilde{L}_{L,3}} &= m^2_{\tilde{L}_{L;1,2}} + F^2_\phi \frac{1}{(16\pi^2)^2}\left[y_\tau^2 \tilde{G}_{y_\tau}\right], \\
m^2_{\tilde{E}^c_{L,3}} &= m^2_{\tilde{E}^c_{L;1,2}} + F^2_\phi \frac{1}{(16\pi^2)^2}\left[2y_\tau^2 \tilde{G}_{y_\tau}\right],
\end{aligned} \tag{28}$$

within which we also include the top, bottom and tau Yukawa contributions. Such contributions can not be neglected at large values of $\tan\beta$.

Expression of the soft m_S^2 receives both anomaly mediation, Yukawa mediation, and interference contributions

$$m_S^2 = \Delta_a m_S^2 + \Delta_Y m_S^2 , \tag{29}$$

with the pure anomaly mediation part being

$$\Delta_a m_S^2 = \frac{F^2_\phi}{(16\pi^2)^2}\left[2\lambda^2 \tilde{G}_\lambda + 2\kappa^2 \tilde{G}_\kappa\right], \tag{30}$$

and the Yukawa deflection part (including the interference terms) being

$$\begin{aligned}
\Delta_Y m_S^2 &= \frac{F^2_\phi}{(16\pi^2)^2}\left\{ d^2 \sum_{i=1}^{N} (5\lambda^2_{S;i} G^+_{\lambda_{S;i}}) - (d^2+2d)\left[2\lambda^2 \Delta\tilde{G}_\lambda + 2\kappa^2 \Delta\tilde{G}_\kappa\right]\right\}, \\
G^+_{\lambda_{S;a}} &= 5(\sum_{j=1}^{N} \lambda^2_{S;j}) + (\lambda^2_{X;a} + \lambda^2_{S;a}) + (\lambda^2_{X;a+1} + \lambda^2_{S;a}) .
\end{aligned} \tag{31}$$

3. Joint Explanation of Muon and Electron $g-2$ Anomaly

We would like to give a joint explanation of muon and electron $g-2$ anomalies in the NMSSM framework from deflected AMSB, taking into account all other low-energy experimental data/exclusion bounds. The SUSY contributions to muon $g-2$ are dominated by the chargino–sneutrino and the neutralino–smuon loop, and the corresponding Feynman diagrams are shown in Figure 1 [72].

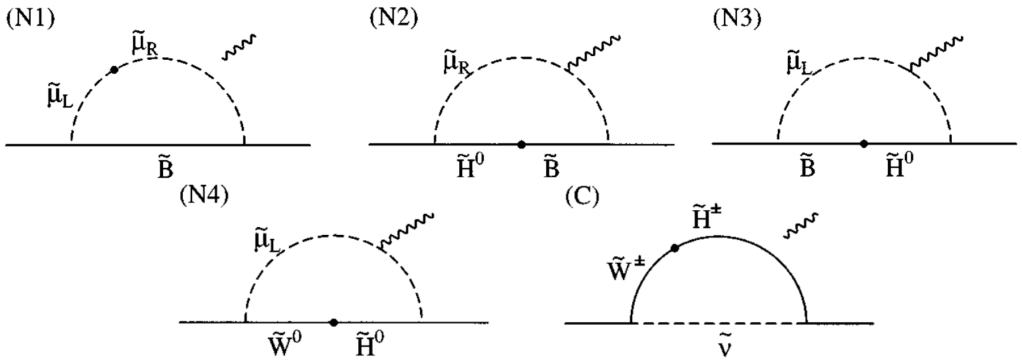

Figure 1. Leading SUSY contributions to Δa_μ [72].

At the leading order of $\tan\beta$ and m_W/m_{SUSY}, they are evaluated as [73]

$$\Delta a_\mu(\tilde{\mu}_L, \tilde{\mu}_R, \tilde{B}) = \frac{\alpha_Y}{4\pi}\frac{m_\mu^2 M_1 \mu}{m^2_{\tilde{\mu}_L} m^2_{\tilde{\mu}_R}} \tan\beta \cdot f_N\left(\frac{m^2_{\tilde{\mu}_L}}{M_1^2}, \frac{m^2_{\tilde{\mu}_R}}{M_1^2}\right). \tag{32}$$

$$\Delta a_\mu(\tilde{B}, \tilde{H}, \tilde{\mu}_R) = -\frac{\alpha_Y}{4\pi}\frac{m_\mu^2}{M_1 \mu} \tan\beta \cdot f_N\left(\frac{M_1^2}{m^2_{\tilde{\mu}_R}}, \frac{\mu^2}{m^2_{\tilde{\mu}_R}}\right), \tag{33}$$

$$\Delta a_\mu(\tilde{B}, \tilde{H}, \tilde{\mu}_L) = \frac{\alpha_Y}{8\pi}\frac{m_\mu^2}{M_1 \mu} \tan\beta \cdot f_N\left(\frac{M_1^2}{m^2_{\tilde{\mu}_L}}, \frac{\mu^2}{m^2_{\tilde{\mu}_L}}\right), \tag{34}$$

$$\Delta a_\mu(\tilde{W}, \tilde{H}, \tilde{\mu}_L) = -\frac{\alpha_2}{8\pi}\frac{m_\mu^2}{M_2 \mu} \tan\beta \cdot f_N\left(\frac{M_2^2}{m^2_{\tilde{\mu}_L}}, \frac{\mu^2}{m^2_{\tilde{\mu}_L}}\right), \tag{35}$$

$$\Delta a_\mu(\tilde{W}, \tilde{H}, \tilde{\nu}_\mu) = \frac{\alpha_2}{4\pi}\frac{m_\mu^2}{M_2 \mu} \tan\beta \cdot f_C\left(\frac{M_2^2}{m^2_{\tilde{\nu}}}, \frac{\mu^2}{m^2_{\tilde{\nu}}}\right), \tag{36}$$

Here, m_μ is the muon mass, m_{SUSY} the SUSY breaking masses and μ the Higgsino mass, respectively. The loop functions are defined as

$$f_C(x,y) = xy\left[\frac{5-3(x+y)+xy}{(x-1)^2(y-1)^2} - \frac{2\log x}{(x-y)(x-1)^3} + \frac{2\log y}{(x-y)(y-1)^3}\right], \tag{37}$$

$$f_N(x,y) = xy\left[\frac{-3+x+y+xy}{(x-1)^2(y-1)^2} + \frac{2x\log x}{(x-y)(x-1)^3} - \frac{2y\log y}{(x-y)(y-1)^3}\right], \tag{38}$$

which are monochromatically increasing for $x > 0, y > 0$ and satisfy $0 \leq f_{C,N}(x,y) \leq 1$. They satisfy $f_C(1,1) = 1/2$ and $f_N(1,1) = 1/6$ in the limit of degenerate masses. The SUSY contributions to the muon $g-2$ will be enhanced for small soft SUSY breaking masses and large value of $\tan\beta$. Similar expressions are evident for electron $g-2$ after properly replacing the couplings and mass parameters for muon by those for electrons. The inclusion of the singlino component in NMSSM will not give sizable contributions to Δa_μ because of the suppressed coupling of singlino to the MSSM sector. However, the lightest neutral CP-odd Higgs scalar could give non-negligible contributions to a_μ if it is quite light [74]. The positive two-loop contribution is numerically more important for a light CP-odd Higgs at approximately 3 GeV and the sum of both one loop and two loop contributions is maximal around $m_{a_1}\sim$6 GeV.

It is non-trivial to jointly explain both muon and electron $g-2$ anomalies in a single framework. The joint explanation of muon and electron $g-2$ anomalies with a negative center value for Δa_e needs either large non-universal trilinear A-terms [47,75] or flavor violating off-diagonal elements in the slepton mass matrices [40,47]. Without explicit flavor mixings, the two anomalies can also be explained by arranging the bino–slepton and chargino–sneutrino contributions differently between the electron and muon sectors, requiring heavy left-hand smuon [39] or light selectrons, wino, and heavy higgsino [42]. Without large flavor violation in the lepton sector, we anticipate that the new physics contributions to the leptonic $g-2$ will, in general, scale with the corresponding lepton square masses. Although such scaling solutions cannot explain the electron $g-2$ data in (3) with negative central value to 2σ range, it, however, can be consistent with the most accurate data in (4) with a positive central value. In our model, universal soft SUSY breaking parameters are predicted for the muon and the electron sector at the messenger scale. Two loop RGE running will only split slightly the low energy spectrum for the two sectors at the SUSY scale. Therefore, we anticipate that the scaling solution will approximately hold in our case.

We use NMSSMTools 5.6.2 [61,76] to scan the whole parameter space to find the desired parameter regions that can account for the muon and electron $g-2$ anomaly. In our numerical calculations, the choices $N = 1$ and $\lambda_{X;a} = \lambda_X, \lambda_{S;a} = \lambda_S$ are adopted for simply. In addition, although there are three new free parameters in the GNMSSM superpotential

in comparison to Z_3 invariant NMSSM, we adopt the most predictive choice with only vanishing ξ_F and other parameters $\hat{\mu} = \mu' = 0$. Non-vanishing ξ_F will lead to additional tadpole terms for S and alter the values of $\langle s \rangle$, $\langle h_u \rangle$, and $\langle h_d \rangle$ for the EWSB minima.

The ranges of the input parameters at the messenger scale M_{mess} are chosen to satisfy

$$10^5 \text{ GeV} < M_{mess} < 10^{15} \text{ GeV},\ 30 \text{ TeV} < F_\phi < 500 \text{ TeV},\ -5 < d < 5,\ 0 \leq \xi_F \leq F_\phi\ ,$$
$$0 < |\kappa|, \lambda < 0.7 \quad \text{with } \lambda^2 + \kappa^2 \lesssim 0.7,\ 0 < \lambda_X, \lambda_S < \sqrt{4\pi},$$

with $F_\phi \ll M_{mess}$. Below the messenger scale, the heavy messenger fields are integrated out and the corresponding RGE trajectory reduces to ordinary GNMSSM type, which can be seen to be deflected from the ordinary AMSB trajectory [48,51] and can, possibly, push the tachyonic slepton masses to positive values. So, the renormalization group equations of GNMSSM [61] are used to evolve the soft SUSY parameters from the messenger scale to the EW scale.

We also impose the following constraints from low energy experimental data other than that already encoded in the NMSSMTools package

(i) The CP-even component S_2 in the Goldstone-'*eaten*' combination of H_u and H_d doublets corresponds to the SM Higgs. Such an S_2 dominated CP-even scalar should lie in the combined mass range for the Higgs boson, 122 GeV $< M_h <$ 128 GeV [1,2]. Note that the uncertainty is 3 GeV instead of default 2 GeV because large λ may induce additional $\mathcal{O}(1)$ GeV correction to M_h at the two-loop level [77].

(ii) Direct search bounds for low mass and high mass resonances at LEP, Tevatron, and LHC by using the package HiggsBounds-5.5.0 [78].

(iii) Constraints on gluino and squark masses from the latest LHC data [79–82] and the lower mass bounds of charginos and sleptons from the LEP [83] results.

(iv) Constraints from B physics, such as $B \to X_s\gamma$, $B_s \to \mu^+\mu^-$and $B^+ \to \tau^+\nu_\tau$, etc. [84–87]

$$3.15 \times 10^{-4} < \quad Br(B_s \to X_s\gamma) \quad < 3.71 \times 10^{-4}\ , \tag{39}$$
$$1.7 \times 10^{-9} < \quad Br(B_s \to \mu^+\mu^-) \quad < 4.5 \times 10^{-9}\ , \tag{40}$$
$$0.78 \times 10^{-4} < \quad Br(B^+ \to \tau^+\nu_\tau) \quad < 1.44 \times 10^{-4}\ . \tag{41}$$

(v) Vacuum stability constraints on the soft SUSY breaking parameters adopted in [12], including the semi-analytic bounds for non-existence of a deeper charge/color breaking (CCB) minimum [88] and/or a meta-stable EW vacuum with a tunneling lifetime longer than the age of the universe [89].
A sufficient condition to ensure vacuum stability at the EW scale is the requirement that EW vacuum is the global minimum (true vacuum) of the scalar potential. If the EW vacuum is a local minimum (false vacuum), the relevant parameter regions can still be allowed if the false EW vacuum is meta-stable with a lifetime longer than the age of the universe.

(vi) The relic density of the dark matter should satisfy the Planck result $\Omega_{DM}h^2 = 0.1199 \pm 0.0027$ [90] in combination with the WMAP data [91] (with a 10% theoretical uncertainty).

We have the following discussions on our numerical results.

- Although it is fairly non-trivial to realize successful EWSB in NMSSM from predictive UV-completion models, for example in ordinary GMSB, numerical scan indicates that some parameter points can still survive the EWSB conditions in our case. In fact, additional couplings in the superpotential involving the singlet S and messengers can change the AMSB predictions of m_S^2 and A_λ, A_κ so as that the necessary condition $A_\kappa^2 \gtrsim 9m_S^2$ for $\langle s \rangle \neq 0$ and other EWSB conditions can be satisfied. The values of $\tan\beta$ at the EW scale can be obtained iteratively after we minimize the scalar potential to obtain $\langle s \rangle$. The allowed values of λ, κ and the corresponding μ_{eff} are shown in the left panel of Figure 2. We can see that the allowed values of λ and κ are always not large.

The dependence of ξ_F versus the low scale $\tan\beta$ are also shown in the right panel of Figure 2. An interesting observation is that successful EWSB can still be allowed with $\xi_F = 0$, which is just the Z_3-invariant NMSSM case.

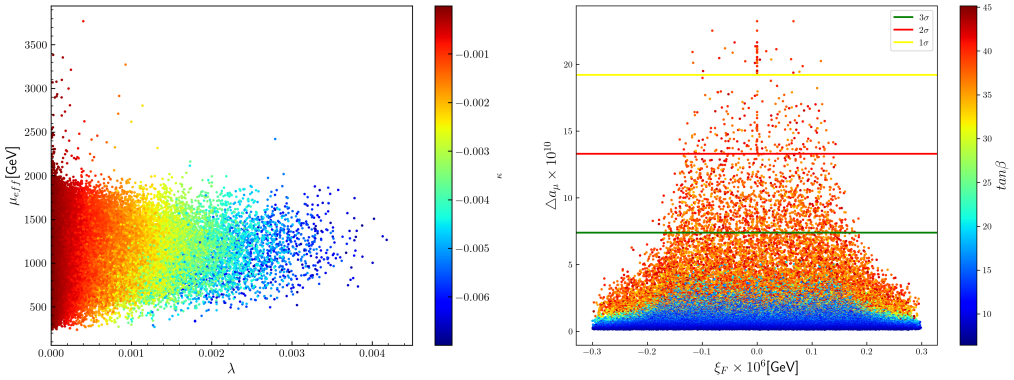

Figure 2. Survived points that can satisfy the constraints (i–vi). The allowed ranges of λ versus μ_{eff}, κ are shown in the **left panel** while the values of ξ_F versus Δa_μ, $\tan\beta$ are shown in the **right panel**.

- From our numerical results, we can see in the right panel of Figure 3 that the muon $g-2$ anomaly can be explained to 1σ range. As noted previously, small flavor violation in the lepton sector will predict that Δa_e and Δa_μ satisfy the scaling relation

$$\frac{\Delta a_e}{\Delta a_\mu} \sim \frac{m_e^2}{m_\mu^2} \sim 2.4 \times 10^{-5}\,, \tag{42}$$

which predicts the same sign of Δa_e as that of Δa_μ. An explanation of the muon $g-2$ anomaly can also lead to the explanation of the electron $g-2$ anomaly in 2σ range for positive central value electron $g-2$ experimental data in (3). Figure 3 shows a scatter plot of Δa_e and Δa_μ with the corresponding SM-like Higgs masses in different colors, as the SM-like Higgs mass always exclude a large portion of otherwise allowed parameter regions. From (42), due to their dependences on the square of the corresponding lepton masses, Δa_e can be seen to be of order 10^{-14} when $\Delta a_\mu \sim \mathcal{O}(10^{-9})$. However, $\Delta a_e \sim \mathcal{O}(10^{-14})$ leads to an apparent horizontal line, when the plot for Δa_e versus Δa_μ is shown in Figure 3.

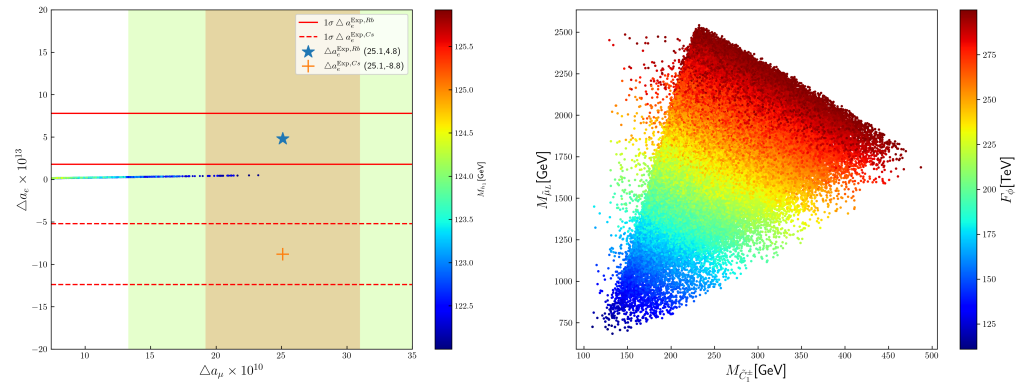

Figure 3. In the **left panel**, we plot the SUSY contributions to Δa_μ versus Δa_e in our case. The red, green, and white areas represent the 1σ, 2σ, and 3σ ranges of Δa_μ, respectively. The positive center value case and negative center value case of electron $g-2$ experimental data are shown with '★' and '+', respectively. The slepton masses versus the chargino masses are shown in the **right panel**.

The NMSSM specific contributions to $\Delta a_{\mu,e}$ are dominantly given by the Barr–Zee type two-loop contributions involving the lightest CP-odd scalar a_1. However, our

numerical results indicate that the a_1 relevant NMSSM specific contributions to $\Delta a_{\mu,e}$ are always small and subdominant.

The plot of the SUSY contributions to muon anomalous magnetic momentum Δa_μ versus the ξ_F parameter are shown in the right panel of Figure 2. It can also be seen from the panel that the Z_3-invariant NMSSM case, which corresponds to $\xi_F = 0$, can also explain the muon $g-2$ anomaly to 1σ range (and the electron $g-2$ anomaly to 2σ range by scaling relations).

- The left panel of Figure 4 shows the plot of the SUSY contributions to muon anomalous magnetic momentum Δa_μ versus the gluino mass $M_{\tilde{g}}$. In AMSB-type scenarios, the F_ϕ parameter determines the mass scales of all the soft SUSY breaking parameters. The larger the value of F_ϕ, the heavier the sfermion and the gaugino masses. We know that light sleptons and electroweakinoes with masses below 0.5∼1 TeV are preferred to explain the muon/electron $g-2$ anomaly via chargino–sneutrino and the neutralino–smuon loops. So, the SUSY explanations of muon/electron $g-2$ anomalies prefer smaller F_ϕ, consequently imposing an upper bounds on the low-energy sparticle masses. Our numerical results show that the gluino masses are bounded to lie 3.5 TeV $\leq M_{\tilde{g}} \leq$ 6.0 TeV if the muon $g-2$ anomaly is explained upon 3σ range. Gluino masses upon 3.5 TeV can possibly be discovered in the future 100 TeV FCC-hh collider.

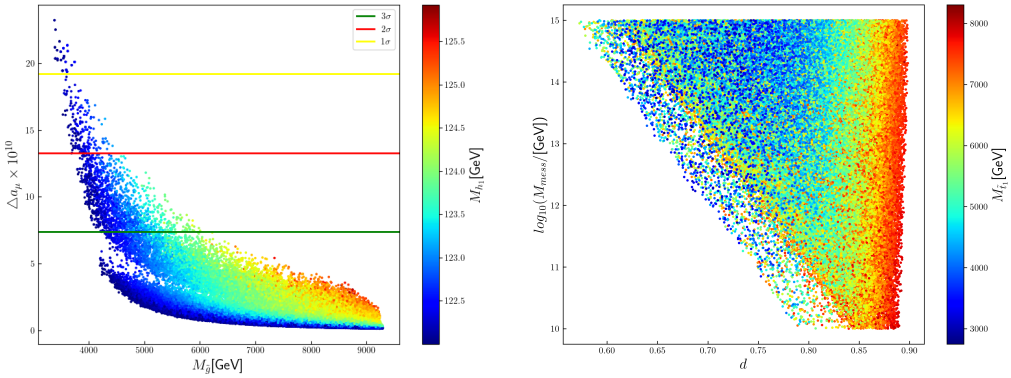

Figure 4. The SUSY contributions to the muon anomalous magnetic momentum Δa_μ versus the gluino mass $M_{\tilde{g}}$ (and the SM-like Higgs mass M_{h_1}) are shown in the **left panel**. The deflection parameter d versus the messenger scale M_{mess}, etc., are shown in the **right panel**.

In mSUGRA type models with universal gaugino masses at the GUT scale or GMSB type models, the gaugino ratios at the EW scale are always given by M_1:M_2:$M_3 \approx$ 1:2:6. Given the LHC exclusion bound 2.2 TeV for $M_{\tilde{g}}$ by LHC, such gaugino ratios are not consistent with very light electroweakinoes, making the explanations of the muon $g-2$ anomaly rather hard. In our case, the gaugino mass ratios change approximately to M_1:M_2:$M_3 \approx (6.6-2d)$:$2(1-2d)$:$6(-3-2d)$ at the EW scale. Therefore, with a proper range of deflection parameter d, the gluino mass can be heavy without contradicting the requirements of light electroweakinoes by the explanation of the muon $g-2$ anomaly. We should note that a positive deflection parameter d is always favored to solve the tachyonic slepton problem for few messenger species in deflected AMSB. To tune the slepton squared masses to small positive values, the range of d are constrained to lie in a small range. In fact, our numerical results indicate that the deflection parameters, which parameterizes the relative size between the anomaly mediation contributions and the gauge/Yukawa mediation contributions, are constrained to lie $0.55 < d < 0.9$ (see the right panel of Figure 4), allowing the gluino to be heavier than 4 TeV for $\mathcal{O}(100)$ GeV wino.

- It can be seen from the previous figures that the observed SM-like 125 GeV Higgs can be accommodated easily in our model. Additional tree-level contributions to SM-like Higgs mass from NMSSM in general allow much lighter stop masses in comparison

to MSSM. In addition, the trilinear coupling A_t are always predicted to be large in deflected AMSB-type models, which are welcome to give sizeable contributions to the SM-like Higgs mass. Light stops and large A_t can also improve the naturalness measurements of the theory. On the other hand, the positive value of A_t tends to decrease to zero and further to large negative values when it RGE evolves down from high input scale to EW scale [92]. So, the values of A_t at the EW scale may not be large for a mildly large messenger scale M_{mess}, making the A_t contribution to the SM-like Higgs mass not important for some range of M_{mess}. Therefore, the stop masses are always not light because the allowed values of λ are small, leading to small tree-level contributions to the SM-like Higgs mass. It can be seen from Figure 4 that the Higgs mass can be as high as 123.7 GeV (124.5 GeV) and the messenger scale M_{mess} is constrained to be larger than 3×10^{11} GeV (1.2×10^{10} GeV) if the muon $g-2$ anomaly is explained upon 2σ (3σ) level, respectively.

As a comparison, the Higgs mass is upper bounded to be 118 GeV (120 GeV) when the muon $g-2$ anomaly is explained at 2σ (3σ) level in the CMSSM/mSUGRA, because light sleptons also indicate light stops (with an universal m_0 input at GUT scale), leading to small loop contributions to Higgs masses. So, our deflected AMSB realization of NMSSM is much better in solving the muon $g-2$ anomaly than that of minimal gravity mediation realization of MSSM.

- Our numerical results indicate that the lightest neutralino DM is always wino-like, which can annihilate very efficiently and lead to the under abundance of DM unless the DM particle mass is heavier than 3 TeV. The NMSSM-specific singlino component is negligibly small, which, therefore, will not play an important role in DM annihilation processes. Our numerical results indicate that the DM particle is constrained to be lighter than 500 GeV. Therefore, additional DM components, such as the axino, are always needed to provide enough cosmic DM. We also check (see the figures in Figure 5) that the Spin-Independent (SI) and Spin-Dependent (SD) DM direct detection constraints, for example, the LUX [93], XENON1T [94,95], and PandaX-4T [96,97], can be satisfied for a large portion of survived points.

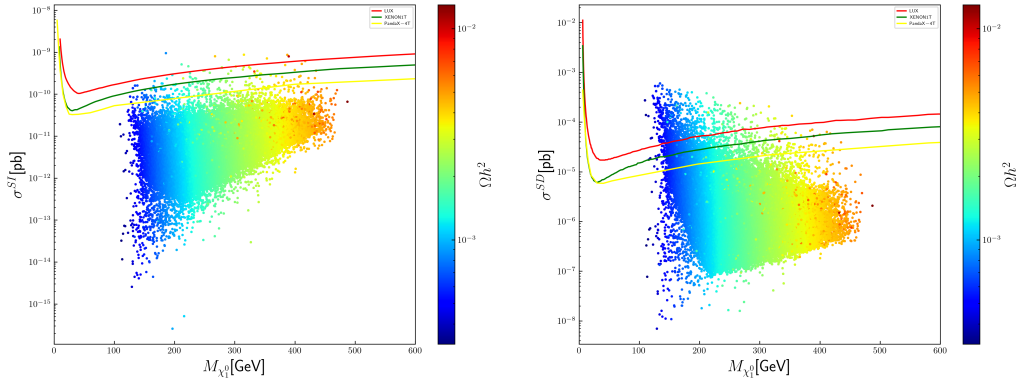

Figure 5. The Spin-Independent (SI) (**left panel**) and Spin-Dependent (SD) (**right panel**) DM direct detection bounds for the survived points. The corresponding DM relic density is shown with different colors.

4. Conclusions

Realistic deflected AMSB-type models are always predictive and can easily lead to light slepton masses when the tachyonic slepton problems that bother them are solved. In addition, the predicted gaugino mass ratios at the EW scale in deflected AMSB are given by M_1:M_2:$M_3 \approx (6.6-2d)$:$2(1-2d)$:$6(-3-2d)$, which are different to the ratios M_1:M_2:$M_3 \approx$ 1:2:6 that appeared in mSUGRA/CMSSM and GMSB. Therefore, much lighter electroweakinoes can still be consistent with the LHC 2.2 TeV gluino lower mass bound. Therefore, the soft SUSY breaking spectrum from deflected AMSB type scenarios with light sleptons and light electroweakinoes are always favored to solve the muon and electron

$g-2$ anomalies. As the AMSB type scenarios always predict insufficient wino-like DM, additional DM species, such as the NMSSM-specific singlino component, can be welcome to provide additional contributions to the DM relic density. Therefore, the embedding of NMSSM framework into realistic AMSB-type UV theory is fairly interesting and well-motivated.

In this paper, we propose to provide a joint explanation of electron and muon $g-2$ anomalies in UV SUSY models in the framework of the anomaly mediation of SUSY breaking. We embed the General NMSSM into the deflected AMSB mechanism with Yukawa/gauge deflection contributions and obtain the relevant soft SUSY breaking spectrum for General NMSSM. After integrated the heavy messenger fields, the analytical expressions of the relevant soft SUSY breaking spectrum for General NMSSM at the messenger scale can be calculated, which can be RGE evolved to EW scale with GNMSSM RGE equations. Our numerical scan indicates that successful EWSB and realistic low-energy NMSSM spectrum can be obtained in some parameter regions. Furthermore, we find that, adopting the positively central value electron $g-2$ experimental data, it is possible to jointly explain the muon $g-2$ anomaly and the electron $g-2$ anomaly within a range of 1σ and 2σ, respectively. The Z_3 invariant NMSSM, which corresponds to $\xi_F = 0$ in our case, can also jointly explain the muon and electron anomaly to 1σ and 2σ range, respectively.

Author Contributions: Conceptualization, F.W.; methodology, F.W. and Z.L.; software, L.J. and Z.L.; validation, F.W.; formal analysis, Z.L.; investigation, L.J.; resources, Z.L.; data curation, L.J.; writing—original draft preparation, F.W.; writing—review and editing, F.W. and Z.L.; visualization, L.J.; supervision, F.W.; project administration, F.W.; funding acquisition, F.W. All authors have read and agreed to the published version of the manuscript.

Funding: This work was supported by the Natural Science Foundation of China under grant numbers 12075213; by the Key Research Project of Henan Education Department for colleges and universities under grant number 21A140025, by the National Supercomputing Center in Zhengzhou.

Data Availability Statement: This manuscript has no associated data or the data will not be deposited. [Authors' comment: Data will be made available on request.]

Conflicts of Interest: The authors declare no conflict of interest.

References

1. Aad, G. et al. [ATLAS]. Combined search for the Standard Model Higgs boson using up to 4.9 fb^{-1} of pp collision data at $\sqrt{s} = 7$ TeV with the ATLAS detector at the LHC. *Phys. Lett. B* **2012**, *710*, 49–66. [CrossRef]
2. Chatrchyan, S. et al. [CMS]. Combined results of searches for the standard model Higgs boson in pp collisions at $\sqrt{s} = 7$ TeV. *Phys. Lett. B* **2012**, *710*, 26–48. [CrossRef]
3. Bennett, G.W. et al. [Muon g-2]. Final Report of the Muon E821 Anomalous Magnetic Moment Measurement at BNL. *Phys. Rev. D* **2006**, *73*, 072003. [CrossRef]
4. Zyla, P.A. et al. [Particle Data Group]. Review of Particle Physics. *Prog. Theor. Exp. Phys.* **2020**, *2020*, 083C01. [CrossRef]
5. Abi, B. et al. [Muon g-2]. Measurement of the Positive Muon Anomalous Magnetic Moment to 0.46 ppm. *Phys. Rev. Lett.* **2021**, *126*, 141801. [CrossRef] [PubMed]
6. Aoyama, T.; Asmussen, N.; Benayoun, M.; Bijnens, J.; Blum, T.; Bruno, M.; Caprini, I.; Calame, C.M.C.; Cè, M.; Colangelo, G.; et al. The anomalous magnetic moment of the muon in the Standard Model. *Phys. Rep.* **2020**, *887*, 1–166. [CrossRef]
7. Parker, R.H.; Yu, C.; Zhong, W.; Estey, B.; Müller, H. Measurement of the fine-structure constant as a test of the Standard Model. *Science* **2018**, *360*, 191–195. [CrossRef]
8. Hanneke, D.; Fogwell, S.; Gabrielse, G. New Measurement of the Electron Magnetic Moment and the Fine Structure Constant. *Phys. Rev. Lett.* **2008**, *100*, 120801. [CrossRef]
9. Aoyama, T.; Kinoshita, T.; Nio, M. Theory of the anomalous magnetic moment of the electron. *Atoms* **2019**, *7*, 28. [CrossRef]
10. Morel, L.; Yao, Z.; Cladé, P.; Guellati-Khélifa, S. Determination of the fine-structure constant with an accuracy of 81 parts per trillion. *Nature* **2020**, *588*, 61–65. [CrossRef] [PubMed]
11. Athron, P.; Balázs, C.; Jacob, D.H.J.; Kotlarski, W.; Stöckinger, D.; Stöckinger-Kim, H. New physics explanations of a_μ in light of the FNAL muon $g-2$ measurement. *J. High Energy Phys.* **2021**, *9*, 80. [CrossRef]
12. Du, X.K.; Li, Z.; Wang, F.; Zhang, Y.K. The muon $g-2$ anomaly in EOGM with adjoint messengers. *Nucl. Phys. B* **2023**, *989*, 116151. [CrossRef]
13. Li, Z.; Liu, G.L.; Wang, F.; Yang, J.M.; Zhang, Y. Gluino-SUGRA scenarios in light of FNAL muon g – 2 anomaly. *J. High Energy Phys.* **2021**, *2021*, 219. [CrossRef]

14. Crivellin, A.; Hoferichter, M. Consequences of chirally enhanced explanations of $(g-2)_\mu$ for h $\to \mu\mu$ and Z $\to \mu\mu$. *J. High Energy Phys.* **2021**, *2021*, 135; Erratum in *J. High Energy Phys.* **2022**, *10*, 30. [CrossRef]
15. Endo, M.; Hamaguchi, K.; Iwamoto, S.; Kitahara, T. Supersymmetric interpretation of the muon g – 2 anomaly. *J. High Energy Phys.* **2021**, *2021*, 75. [CrossRef]
16. Gu, Y.; Liu, N.; Su, L.; Wang, D. Heavy bino and slepton for muon $g-2$ anomaly. *Nucl. Phys. B* **2021**, *969*, 115481. [CrossRef]
17. Van Beekveld, M.; Beenakker, W.; Schutten, M.; De Wit, J. Dark matter, fine-tuning and $(g-2)_\mu$ in the pMSSM. *SciPost Phys.* **2021**, *11*, 049. [CrossRef]
18. Yin, W. Muon $g-2$ anomaly in anomaly mediation. *J. High Energy Phys.* **2021**, *2021*, 29. [CrossRef]
19. Abdughani, M.; Fan, Y.Z.; Feng, L.; Tsai, Y.L.S.; Wu, L.; Yuan, Q. A common origin of muon $g-2$ anomaly, Galaxy Center GeV excess and AMS-02 anti-proton excess in the NMSSM. *Sci. Bull.* **2021**, *66*, 2170–2174. [CrossRef]
20. Cao, J.; Lian, J.; Pan, Y.; Zhang, D.; Zhu, P. Improved $(g-2)_\mu$ measurement and singlino dark matter in μ-term extended $\mathbb{Z}_3$-NMSSM. *J. High Energy Phys.* **2021**, *2021*, 175. [CrossRef]
21. Wang, F.; Wang, W.; Yang, J.M.; Zhang, Y. Heavy colored SUSY partners from deflected anomaly mediation. *J. High Energy Phys.* **2015**, *2015*, 138. [CrossRef]
22. Wang, F.; Wu, L.; Xiao, Y.; Yang, J.M.; Zhang, Y. GUT-scale constrained SUSY in light of new muon $g-2$ measurement. *Nucl. Phys. B* **2021**, *970*, 115486. [CrossRef]
23. Cox, P.; Han, C.; Yanagida, T.T. Muon $g-2$ and dark matter in the minimal supersymmetric standard model. *Phys. Rev. D* **2018**, *98*, 055015. [CrossRef]
24. Yang, J.M.; Zhang, Y. Low energy SUSY confronted with new measurements of W-boson mass and muon g-2. *Sci. Bull.* **2022**, *67*, 1430–1436. [CrossRef]
25. Cox, P.; Han, C.; Yanagida, T.T. Muon $g-2$ and coannihilating dark matter in the minimal supersymmetric standard model. *Phys. Rev. D* **2021**, *104*, 075035. [CrossRef]
26. Han, C. Muon g $-$ 2 and CP violation in MSSM. *arXiv* **2021**, arXiv:2104.03292.
27. Baum, S.; Carena, M.; Shah, N.R.; Wagner, C.E.M. The tiny (g-2) muon wobble from small-μ supersymmetry. *J. High Energy Phys.* **2022**, *2022*, 25. [CrossRef]
28. Zhang, H.B.; Liu, C.X.; Yang, J.L.; Feng, T.F. Muon anomalous magnetic dipole moment in the μ νSSM *. *Chin. Phys. C* **2022**, *46*, 093107. [CrossRef]
29. Ahmed, W.; Khan, I.; Li, J.; Li, T.; Raza, S.; Zhang, W. The natural explanation of the muon anomalous magnetic moment via the electroweak supersymmetry from the GmSUGRA in the MSSM. *Phys. Lett. B* **2022**, *827*, 136879. [CrossRef]
30. Yang, J.L.; Zhang, H.B.; Liu, C.X.; Dong, X.X.; Feng, T.F. Muon $(g-2)$ in the B-LSSM. *J. High Energy Phys.* **2021**, *2021*, 86. [CrossRef]
31. Aboubrahim, A.; Klasen, M.; Nath, P. What the Fermilab muon $g-2$ experiment tells us about discovering supersymmetry at high luminosity and high energy upgrades to the LHC. *Phys. Rev. D* **2021**, *104*, 035039. [CrossRef]
32. Chakraborti, M.; Roszkowski, L.; Trojanowski, S. GUT-constrained supersymmetry and dark matter in light of the new $(g-2)_\mu$ determination. *J. High Energy Phys.* **2021**, *2021*, 252. [CrossRef]
33. Baer, H.; Barger, V.; Serce, H. Anomalous muon magnetic moment, supersymmetry, naturalness, LHC search limits and the landscape. *Phys. Lett. B* **2021**, *820*, 136480. [CrossRef]
34. Altmannshofer, W.; Gadam, S.A.; Gori, S.; Hamer, N. Explaining $(g-2)_\mu$ with multi-TeV sleptons. *J. High Energy Phys.* **2021**, *2021*, 118. [CrossRef]
35. Aboubrahim, A.; Nath, P.; Syed, R.M. Yukawa coupling unification in an SO(10) model consistent with Fermilab $(g-2)_\mu$ result. *J. High Energy Phys.* **2021**, *2021*, 2. [CrossRef]
36. Zhang, Z.N.; Zhang, H.B.; Yang, J.L.; Zhao, S.M.; Feng, T.F. Higgs boson decays with lepton flavor violation in the $B-L$ symmetric SSM. *Phys. Rev. D* **2021**, *103*, 115015. [CrossRef]
37. Jeong, K.S.; Kawamura, J.; Park, C.B. Mixed modulus and anomaly mediation in light of the muon $g-2$ anomaly. *J. High Energy Phys.* **2021**, *2021*, 64. [CrossRef]
38. Abdughani, M.; Hikasa, K.I.; Wu, L.; Yang, J.M.; Zhao, J. Testing electroweak SUSY for muon $g-2$ and dark matter at the LHC and beyond. *J. High Energy Phys.* **2019**, *2019*, 95. [CrossRef]
39. Li, S.; Xiao, Y.; Yang, J.M. Can electron and muon $g-2$ anomalies be jointly explained in SUSY?. *Eur. Phys. J. C* **2022**, *82*, 276. [CrossRef]
40. Dutta, B.; Mimura, Y. Electron $g-2$ with flavor violation in MSSM. *Phys. Lett. B* **2019**, *790*, 563–567. [CrossRef]
41. Baldini, A.M. et al. [MEG]. Search for the lepton flavour violating decay $\mu^+ \to e^+\gamma$ with the full dataset of the MEG experiment. *Eur. Phys. J. C* **2016**, *76*, 434. [CrossRef]
42. Badziak, M.; Sakurai, K. Explanation of electron and muon $g-2$ anomalies in the MSSM. *J. High Energy Phys.* **2019**, *2019*, 24. [CrossRef]
43. Endo, M.; Yin, W. Explaining electron and muon $g-2$ anomaly in SUSY without lepton-flavor mixings. *J. High Energy Phys.* **2019**, *2019*, 122. [CrossRef]
44. Ali, M.I.; Chakraborti, M.; Chattopadhyay, U.; Mukherjee, S. Muon and electron $(g-2)$ anomalies with non-holomorphic interactions in MSSM. *Eur. Phys. J. C* **2023**, *83*, 60. [CrossRef]
45. Yang, J.L.; Feng, T.F.; Zhang, H.B. Electron and muon $(g-2)$ in the B-LSSM. *J. Phys. G* **2020**, *47*, 055004. [CrossRef]

46. Cao, J.; He, Y.; Lian, J.; Zhang, D.; Zhu, P. Electron and muon anomalous magnetic moments in the inverse seesaw extended NMSSM. *Phys. Rev. D* **2021**, *104*, 055009. [CrossRef]
47. Li, S.; Li, Z.; Wang, F.; Yang, J.M. Explanation of electron and muon $g-2$ anomalies in AMSB. *Nucl. Phys. B* **2022**, *983*, 115927. [CrossRef]
48. Randall, L.; Sundrum, R. Out of this world supersymmetry breaking. *Nucl. Phys. B* **1999**, *557*, 79–118. [CrossRef]
49. Giudice, G.F.; Luty, M.A.; Murayama, H.; Rattazzi, R. Gaugino mass without singlets. *J. High Energy Phys.* **1998**, *12*, 027. [CrossRef]
50. Jack, I.; Jones, D.R.T. RG invariant solutions for the soft supersymmetry breaking parameters. *Phys. Lett. B* **1999**, *465*, 148–154. [CrossRef]
51. Pomarol, A.; Rattazzi, R. Sparticle masses from the superconformal anomaly. *J. High Energy Phys.* **1999**, *1999*, 013. [CrossRef]
52. Rattazzi, R.; Strumia, A.; Wells, J.D. Phenomenology of deflected anomaly mediation. *Nucl. Phys. B* **2000**, *576*, 3–28. [CrossRef]
53. Okada, N.; Positively deflected anomaly mediation. *Phys. Rev. D* **2002**, *65*, 115009. [CrossRef]
54. Okada, N.; Tran, H.M. Positively deflected anomaly mediation in the light of the Higgs boson discovery. *Phys. Rev. D* **2013**, *87*, 035024. [CrossRef]
55. Wang, F. Deflected anomaly mediated SUSY breaking scenario with general messenger–matter interactions. *Phys. Lett. B* **2015**, *751*, 402–407. [CrossRef]
56. Ellwanger, U.; Hugonie, C.; Teixeira, A.M. The Next-to-Minimal Supersymmetric Standard Model. *Phys. Rep.* **2010**, *496*, 1–77. [CrossRef]
57. Maniatis, M. The Next-to-Minimal Supersymmetric extension of the Standard Model reviewed. *Int. J. Mod. Phys. A* **2010**, *25*, 3505–3602. [CrossRef]
58. Giudice, G.F.; Rattazzi, R. Theories with gauge-mediated supersymmetry breaking. *Phys. Rep.* **1999**, *322*, 419–499. [CrossRef]
59. Dine, M.; Fischler, W.; Srednicki, M. Supersymmetric Technicolor. *Nucl. Phys. B* **1981**, *189*, 575. [CrossRef]
60. de Gouvea, A.; Friedland, A.; Murayama, H. Next-to-minimal supersymmetric standard model with the gauge mediation of supersymmetry breaking. *Phys. Rev. D* **1998**, *57*, 5676–5696. [CrossRef]
61. Ellwanger, U.; Jean-Louis, C.C.; Teixeira, A.M. Phenomenology of the General NMSSM with Gauge Mediated Supersymmetry Breaking. *J. High Energy Phys.* **2008**, *2008*, 044. [CrossRef]
62. Han, T.; Marfatia, D.; Zhang, R.J. A Gauge mediated supersymmetry breaking model with an extra singlet Higgs field. *Phys. Rev. D* **2000**, *61*, 013007. [CrossRef]
63. Nilles, H.P. Supersymmetry, Supergravity and Particle Physics. *Phys. Rep.* **1984**, *110*, 1–162. [CrossRef]
64. Canepa, A. Searches for Supersymmetry at the Large Hadron Collider. *Rev. Phys.* **2019**, *4*, 100033. [CrossRef]
65. Delgado, A.; Giudice, G.F.; Slavich, P. Dynamical μ term in gauge mediation. *Phys. Lett. B* **2007**, *653*, 424–433. [CrossRef]
66. Giudice, G.F.; Rattazzi, R. Extracting supersymmetry breaking effects from wave function renormalization. *Nucl. Phys. B* **1998**, *511*, 25–44. [CrossRef]
67. Chacko, Z.; Ponton, E. Yukawa deflected gauge mediation. *Phys. Rev. D* **2002**, *66*, 095004. [CrossRef]
68. Wang, F.; Yang, J.M.; Zhang, Y. Radiative natural SUSY spectrum from deflected AMSB scenario with messenger-matter interactions. *J. High Energy Phys.* **2016**, *2016*, 177. [CrossRef]
69. Wang, F.; Wang, W.; Yang, J.M. Solving the muon $g-2$ anomaly in deflected anomaly mediated SUSY breaking with messenger-matter interactions. *Phys. Rev. D* **2017**, *96*, 075025. [CrossRef]
70. Evans, J.A.; Shih, D. Surveying Extended GMSB Models with m_h = 125 GeV. *J. High Energy Phys.* **2013**, *2013*, 93. [CrossRef]
71. Martin, S.P. A Supersymmetry primer. *Adv. Ser. Direct. High Energy Phys.* **1998**, *18*, 1–98. ._0001 [CrossRef]
72. Moroi, T. The Muon anomalous magnetic dipole moment in the minimal supersymmetric standard model. *Phys. Rev. D* **1996**, *53*, 6565–6575; Erratum in *Phys. Rev. D* **1997**, *56*, 4424. [CrossRef]
73. Endo, M.; Hamaguchi, K.; Iwamoto, S.; Yoshinaga, T. Muon g-2 vs LHC in Supersymmetric Models. *J. High Energy Phys.* **2014**, *2014*, 123. [CrossRef]
74. Domingo, F.; Ellwanger, U. Constraints from the Muon $g-2$ on the Parameter Space of the NMSSM. *J. High Energy Phys.* **2008**, *2008*, 79. [CrossRef]
75. Crivellin, A.; Girrbach, J.; Nierste, U. Yukawa coupling and anomalous magnetic moment of the muon: An update for the LHC era. *Phys. Rev. D* **2011**, *83*, 055009. [CrossRef]
76. Allanach, B.C.; Balazs, C.; Belanger, G.; Bernhardt, M.; Boudjema, F.; Choudhury, D.; Desch, K.; Ellwanger, U.; Gambino, P.; Godbole, R.; et al. SUSY Les Houches Accord 2. *Comput. Phys. Commun.* **2009**, *180*, 8–25. [CrossRef]
77. Goodsell, M.D.; Nickel, K.; Staub, F. Two-loop corrections to the Higgs masses in the NMSSM. *Phys. Rev. D* **2015**, *91*, 035021. [CrossRef]
78. Bechtle, P.; Brein, O.; Heinemeyer, S.; Stal, O.; Stefaniak, T.; Weiglein, G.; Williams, K.E. HiggsBounds-4: Improved Tests of Extended Higgs Sectors against Exclusion Bounds from LEP, the Tevatron and the LHC. *Eur. Phys. J. C* **2014**, *74*, 2693. [CrossRef]
79. Heisterkamp, S.J.F. *R*-Hadron Search at ATLAS. Ph.D. Thesis, University of Copenhagen, Copenhagen, Denmark, 2012.
80. [ATLAS]. Measurement of nuclear modification factor for muons from charm and bottom hadrons in Pb+Pb collisions at 5.02 TeV with the ATLAS detector. *Phys. Lett. B* **2022**, *829*, 137077. [CrossRef]
81. [CMS]. Search for top squark pair production in the single lepton final state in pp collisions at $\sqrt{s} = 13$ TeV. *Eur. Phys. J. C* **2013**, *73*, 2677. [CrossRef]

82. [ATLAS]. Search for production of supersymmetric particles in final states with missing transverse momentum and multiple b-jets at $\sqrt{s} = 13$ TeV proton-proton collisions with the ATLAS detector. *J. High Energ. Phys.* **2014**, *2014*, 24. [CrossRef]
83. Schael, S. et al. [ALEPH, DELPHI, L3, OPAL, SLD, LEP Electroweak Working Group, SLD Electroweak Group and SLD Heavy Flavour Group]. Precision electroweak measurements on the *Z* resonance. *Phys. Rep.* **2006**, *427*, 257–454. [CrossRef]
84. Lees, J.P. et al. [BaBar]. Precision Measurement of the $B \to X_s\gamma$ Photon Energy Spectrum, Branching Fraction, and Direct CP Asymmetry $A_{CP}(B \to X_{s+d}\gamma)$. *Phys. Rev. Lett.* **2012**, *109*, 191801. [CrossRef] [PubMed]
85. Lees, J.P. et al. [BaBar]. Evidence for an excess of $\bar{B} \to D^{(*)}\tau^-\bar{\nu}_\tau$ decays. *Phys. Rev. Lett.* **2012**, *109*, 101802. [CrossRef]
86. Aaij, R. et al. [LHCb]. First Evidence for the Decay $B_s^0 \to \mu^+\mu^-$. *Phys. Rev. Lett.* **2013**, *110*, 021801. [CrossRef] [PubMed]
87. Akeroyd, A.G.; Recksiegel, S. The Effect of H+- on B+- —> tau+- nu(tau) and B+- —> mu+- muon neutrino. *J. Phys. G* **2003**, *29*, 2311–2317. [CrossRef]
88. Kitahara, T.; Yoshinaga, T. Stau with Large Mass Difference and Enhancement of the Higgs to Diphoton Decay Rate in the MSSM. *J. High Energy Phys.* **2013**, *2013*, 35. [CrossRef]
89. Casas, J.A.; Lleyda, A.; Munoz, C. Strong constraints on the parameter space of the MSSM from charge and color breaking minima. *Nucl. Phys. B* **1996**, *471*, 3–58. [CrossRef]
90. Ade, P.A.R. et al. [Planck]. Planck 2015 results. XIII. Cosmological parameters. *Astron. Astrophys.* **2016**, *594*, A13. [CrossRef]
91. Dunkley, J. et al. [WMAP]. Five-Year Wilkinson Microwave Anisotropy Probe (WMAP) Observations: Likelihoods and Parameters from the WMAP data. *Astrophys. J. Suppl.* **2009**, *180*, 306–329. [CrossRef]
92. Draper, P.; Meade, P.; Reece, M.; Shih, D. Implications of a 125 GeV Higgs for the MSSM and Low-Scale SUSY Breaking. *Phys. Rev. D* **2012**, *85*, 095007. [CrossRef]
93. Akerib, D.S. et al. [LUX]. Results from a search for dark matter in the complete LUX exposure. *Phys. Rev. Lett.* **2017**, *118*, 021303. [CrossRef] [PubMed]
94. Aprile, E. et al. [XENON]. Dark Matter Search Results from a One Ton-Year Exposure of XENON1T. *Phys. Rev. Lett.* **2018**, *121*, 111302. [CrossRef] [PubMed]
95. Aprile, E. et al. [XENON]. Constraining the spin-dependent WIMP-nucleon cross sections with XENON1T. *Phys. Rev. Lett.* **2019**, *122*, 141301. [CrossRef]
96. Meng, Y. et al. [PandaX-4T]. Dark Matter Search Results from the PandaX-4T Commissioning Run. *Phys. Rev. Lett.* **2021**, *127*, 261802. [CrossRef] [PubMed]
97. Huang, Z. et al. [PandaX]. Constraints on the axial-vector and pseudo-scalar mediated WIMP-nucleus interactions from PandaX-4T experiment. *Phys. Lett. B* **2022**, *834*, 137487. [CrossRef]